Enabling On-Demand Low-Power mmWave Repeaters via Passive Beamforming

Tianxiang Li
UCLA
United States

Mohammad H. Mazaheri
UCLA
United States

Omid Abari
UCLA
United States

ABSTRACT

Advancements in computing have enabled emerging applications such as telesurgery, robot automation, holographic telepresence, and extended reality, which require gigabit-per-second throughput, sub-millisecond latency, and highly reliable wireless connectivity. Millimeter wave (mmWave) technology has promised to enable such connectivity by operating over a large bandwidth in the high-frequency spectrum bands (24 GHz and above). However, due to the short wavelength and high directionality of mmWave signals, mmWave networks have limited coverage and are highly susceptible to blockage. In particular, high-data-rate mmWave networks work reliably only when there is a clear line-of-sight (LOS) path between users and base stations. Unfortunately, due to this problem, mmWave networks have not been able to scale and become ubiquitous. Past work has proposed mmWave repeaters and intelligent surfaces to solve this issue by rerouting signal around blockages. However, these solutions are expensive and complex to build, consume high power, or/and require constant feedback from the network to operate since they use active techniques for beam steering. In this paper, we present the first mmWave repeater which uses passive beamforming technique. Our repeater is low-cost, low-power, and can support multiple users simultaneously. Most importantly, it does not require any feedback from the network to operate. Hence, it can be easily deployed on-demand to solve the coverage and blockage problem of mmWave networks whenever and wherever high-data-rate and low-latency connectivity is needed.

CCS CONCEPTS

• **Hardware** → **Wireless devices**; **Beamforming**.

ACM MobiCom '24, November 18-22, 2024, Washington D.C., DC, USA

ACM ISBN 979-8-4007-0489-5/24/09
https://doi.org/10.1145/3636534.3649385

ACM Reference Format:
Tianxiang Li, Mohammad H. Mazaheri, and Omid Abari. 2024. Enabling On-Demand Low-Power mmWave Repeaters via Passive Beamforming. In *The 30th Annual International Conference on Mobile Computing and Networking (ACM MobiCom '24), September 30-October 4, 2024, Washington D.C., DC, USA.* ACM, New York, NY, USA, 15 pages. https://doi.org/10.1145/3636534.3649385

1 INTRODUCTION

In recent years there has been a growing demand for reliable high data rate and low latency wireless networks due to the popularization of applications such as real-time video streaming, augmented reality (AR), robotic automation, online education, and drone-based video streaming for sporting events [21, 52, 53, 63, 71]. Millimeter wave (mmWave) technology has promised to fulfil this demand by operating in a large high-frequency spectrum (24 GHz and above) [35–38, 44, 49, 50]. In fact, the Federal Communications Commission (FCC) has released more than 14 GHz of bandwidth in the mmWave frequency bands, which is orders of magnitude more than the bandwidth allocated to traditional cellular and WiFi networks [11]. However, existing mmWave networks face a major problem which prevents them from becoming scalable and ubiquitous. mmWave networks have a very limited coverage since they use high-frequency signals which experience a huge path loss. To compensate for this loss, today's mmWave systems use directional antennas and focus the signal power in a narrow beam. Hence, communication between two nodes is possible when their beams are aligned. However, as shown in Figure 1, these beams can be easily blocked by obstacles such as a wall, a person or even furniture, resulting in 20 dB and higher drop in Signal-to-Noise ratio (SNR) [10, 70]. Therefore, mmWave networks cannot provide reliable high-data-rate links in environments with static or mobile obstacles.

To overcome this problem, researchers have designed mmWave relays, repeaters and intelligent surfaces [10, 14, 23, 43, 45, 58]. The vision is to design a device that effectively increases the network coverage and reliability of mmWave networks by relaying and rerouting signals around obstacles, or refocusing it to avoid significant signal power loss. However, existing systems have limitations which hinder their practicality. For example, existing mmWave relays and repeaters either support only a single user or/and require

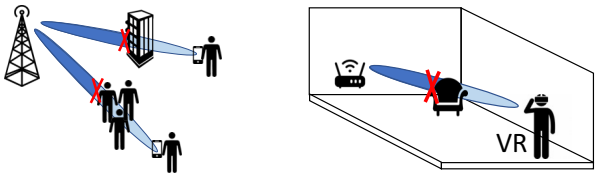

(a) Outdoor (b) Indoor

Figure 1: mmWave networks problem. mmWave signals are directional, and hence they can be blocked by obstacles.

phased arrays which are complex, expensive, and consume significant amount of power [22, 41, 43]. To address the complexity and power consumption of these systems, a new type of repeaters (known as intelligent surfaces) have been proposed. These systems use a large array (a few hundred to thousand elements) of reconfigurable passive elements to refocus and reroute signals [14, 40, 45, 58]. However, they are still costly to manufacture since they require a mmWave component (typically a diode) per each element and high-speed realtime control unit such as field-programmable gate array (FPGA). Most importantly, they require frequent feedback from the base station and the client as they must cooperate with them to work and adjust their beams' direction. Hence, they cannot be deployed seamlessly on-demand without significant changes to the client or base station. Ideally, an mmWave repeater needs to satisfy multiple requirements to effectively achieve the goal of making mmWave networks scalable and ubiquitous:

- *On-demand and Rapid Deployment:* It must work seamlessly with the base stations and clients without requiring any cooperation or feedback from them. This enables on-demand and rapid deployment of the repeater, extending reliable mmWave networks to wherever and whenever needed. For example, during an emergency response, or an event in a part of a city, we can quickly use this repeater and enable high-data-rate low-latency mmWave networks to users.
- *Low-Cost and Low-Power:* Its design and implementation need to be low-power, low-cost, and lightweight, such that it can be battery (or solar) powered, and be easily deployed on a pole or a drone whenever and wherever high-data-rate connectivity is needed.
- *Multi-user Support:* Finally, it needs to provide reliable high-data-rate links to many users. Otherwise, it cannot be used in emerging applications such as multi-user virtual reality, smart home, and stadium augmented reality, where ten to thousands of mobile devices need reliable, high-data-rate, low-latency mmWave connectivity.

If the above requirements are satisfied, we can envision making reliable mmWave networks scalable and ubiquitous. However, to the best of our knowledge, no current system satisfies all of these requirements.

In this paper, we introduce mmXtend, a low-power low-cost repeater system which can be battery (or solar) powered, and be easily deployed on a pole or a drone whenever and wherever high-data-rate connectivity is needed. mmXtend can form and steer beams to multiple users, simultaneously, without requiring phased arrays, or other complex and power hungry hardware such as radios, FPGAs or processors. Moreover, our solution can work seamlessly with the base station and client. Therefore, it can effectively address the coverage limitations of mmWave networks in both outdoor and indoor scenarios whenever and wherever is needed such as crowded events, disaster recovery, smart factories, and smart homes as shown in Figure 2.

To develop mmXtend, we first need to develop a 2D beamforming technique for our repeater. The solution must be low-power, low-cost, and simple to fabricate. Moreover, it needs to allow the base station or client to control the repeater's beams direction without sending any message or feedback to the repeater. To achieve this, we develop a Frequency Scanning Antenna (FSA) operating at mmWave. Our design enables 1D passive beamforming and steering while it can be fabricated using only printed circuit board (PCB). Such a design enables our repeater to perform Frequency Division Multiple Access (FDMA) for users in different directions since FSA creates multiple beams while each radiating only a specific frequency channel. Moreover, since the direction of the beam is a function of the signal frequency, the base station or client can simply steer the repeater beams without its cooperation. We then design a mmWave Rotman lens and integrate it to our FSA design on the same PCB. Rotman lens is a passive structure with multiple ports which enables 1D beamforming where each beam is fed by a different port. Hence, integration of a FSA and Rotman lens enables our repeater to perform 2D beamforming, supporting multiple users in each frequency channels. In particular, by incorporating Multi-User Multiple Input Multiple Output (MU-MIMO) into our design, our repeater can support multi-user in each frequency channel through Space Division Multiple Access (SDMA). Finally, we integrate low-power amplifiers to our design, enabling low-power repeaters which amplifies and refocuses mmWave signals while it can be deployed seamlessly, without requiring any cooperation or feedback from base station or client.

This paper makes the following contributions[1]:

- We introduce mmXtend a new repeater for mmWave networks which is low-cost, low-power, supports multi-user, and can be easily deployed on-demand (without requiring any feedback from the network to operate).

[1]This work does not raise any ethical issues.

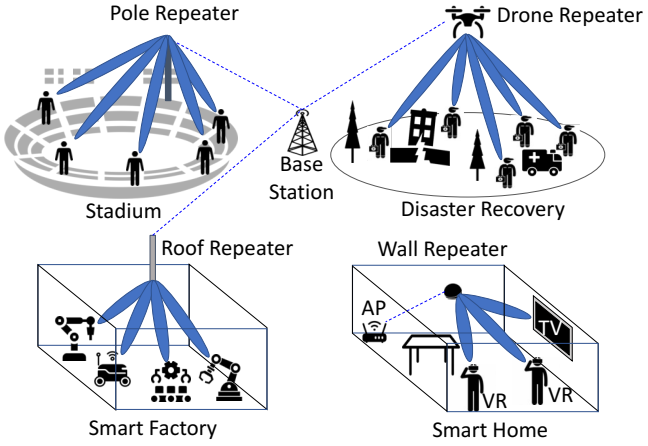

Figure 2: mmXtend applications. Our repeater can be deployed on-demand in outdoor and indoor scenarios, solving the blockage problem of mmWave networks.

- We design a 2D passive beamforming and steering structure which can be easily implemented on printed circuit board (PCB), and operates in the 5G mmWave frequency band of 26.5 GHz to 29.5 GHz. More importantly, we show the applicability of passive beamforming in wireless repeaters for the first time.
- We built mmXtend and empirically evaluated its performance in a variety of scenarios. Our results show that mmXtend solves the blockage problem, and enables data rate of more than 250 Mbps link to each user when there are up to 200 users. Even when there are 3600 users, it can provide each user with a 20 Mbps link, which is sufficient for AR or VR 360 degree 4K video [47].

2 MMXTEND OVERVIEW

mmXtend is a low-power low-cost repeater system which can be battery (or solar) powered, and be easily deployed on a pole or a drone whenever and wherever high-data-rate connectivity is needed, as shown in Figure 2. In a scenario where the line of sight between a base station and a user is blocked, mmXtend receives the signal from the base station and forms and steers beams to the user. mmXtend can support multiple users simultaneously, without requiring phased arrays or other complex and power-hungry circuits. Moreover, our solution works seamlessly with the base stations and users. Hence, it can effectively address the coverage limitations of mmWave networks in both indoor and outdoor environments. To develop and build mmXtend, we need to address multiple challenges. First, we need to design a technique which forms and steers beams to multiple users simultaneously, without consuming any power. Second, we need to extend our beam steering approach to 2D and build a repeater which covers the whole space. Finally, our design needs to seamlessly support protocols for multi-user communication, link establishment, and mobility. In the next few sections, we will explain how we address these challenges, and discuss the components that contribute to the design of mmXtend.

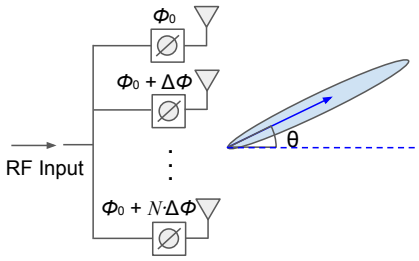

Figure 3: Phased Arrays beamforming and steering.

3 BEAM FORMING AND STEERING

The main challenge in building a low-cost, low-power mmWave repeater is to enable the repeater to create multiple beams simultaneously, while each transmitting a different signal to each user. Although past mmWave work has proposed different approaches for creating and steering one or multiple directional beams, they are not practical for low-power low-cost repeaters since they rely on phased arrays which are complex and consume high power [25, 32, 67]. Below, we discuss some limitations of phased arrays for mmWave repeaters in more detail.

Phased array and its limitations: Phased array consists of an array of fixed-spacing antenna elements, where each antenna is connected to an electronically controlled phase shifter. The radio waves emitted from antennas will combine with each other, forming a narrow beam with stronger signal strength toward a specific direction. By controlling the phase shifters, the amount of phase shift ($\Delta\phi$) between each antenna element can be adjusted which results in a change in the the angle of the beam θ as shown in Figure 3. This enables phased array to form a narrow beam and to electronically steer it in different directions. The main limitation of phased arrays is that it requires calibration and extensive control over the phase shifters which makes the system very complex, power hungry and costly. In particular, repeaters which use phased arrays for beam steering require a processor (such as FPGA) to control the phase shifters and adjust the direction of the beam. Moreover, they need real-time feedback from the client and the base station to steer their beams to the correct direction. Finally, to generate multiple beams simultaneously with independent data streams, phased arrays require multiple transmitter or/and receiver chains. As a result, the required hardware becomes extensively costly and complex, making it unsuitable to be deployed flexibly on-demand at different locations.

Our goal is to develop a low-power, low-cost design that enables the repeater to support multiple users simultaneously (i.e. creating and steering multiple beams in different directions) without using any phased arrays, or requiring any feedback from the base station or clients.

3.1 1D Passive Beam Forming and Steering

To enable low-power, low-cost beam steering and multi-user access, our novel idea is to develop a repeater system based on Frequency Scanning Antenna (FSA) technique. FSA is a technique used primarily in radar imaging and weather forecast to perform measurements [28, 69]. It is a passive structure which focuses and transmits (or receives) a signal toward a direction, where the direction of the signal depends on the frequency of its input signal, as shown in Figure 4. One can design an FSA on PCB consisting of a substrate with many radiating elements (slots). When a signal is fed to the input of the FSA structure, the signal gradually leaks into space through these radiating slots. However, the signal experiences a different phase shift at each radiating slot, which causes the radiated signals to combine constructively in a certain direction, as shown in Figure 4. Since signals of different frequencies have different wavelengths, they experience different amounts of phase shift at each radiating slot. Hence, FSA forms a transmitting beam toward a direction which depends on the frequency of the signal. Note, FSA performs the same for receiving a signal too.

Our idea is that an FSA can provide a passive way to create multiple beams simultaneously when the signal contains multiple channels with different center frequencies. Moreover, we can steer each beam based on the shift in its signal center frequency, without relying on any phase shifters or active components. Hence, by integrating an FSA on a repeater, the repeater can create multiple beams toward the users, simultaneously. In particular, when the base station transmits/receives a signal consisting of multiple frequency channels (centered at f_1 to f_n) to/from the repeater, the FSA on the repeater is able to passively split the different frequency channels into separate high-gain beams to cover different areas on the ground. We note that compared to phase arrays, our design has much lower power, lower complexity, and lower cost for beam steering and creating multiple beams simultaneously since it is purely based on a passive structure. Moreover, it does not require any processor or feedback from the base station (or the client) since they can steer the repeater's beam themselves by changing the frequency channel. In Section 9, we will provide more details on how this design would enable a repeater which can be easily deployed without any need for a change or feedback to the base station or client.

Traditional mmWave FSA designs have multiple limitations which we need to address before using them in our repeater design. First, their designs require a large bandwidth to achieve a wide range of steering angles. Unfortunately, such a large bandwidth is not available in the 5G mmWave band. Second, they only support beam scanning from 0° to positive angles. This is due to the fact that the wave traveling in the structure only provides positive phase shift between consecutive radiating elements. Therefore, for our repeater, we need to design an FSA which (a) requires smaller bandwidth for beam steering and (b) covers negative angles.

(a) Requiring smaller bandwidth for beam steering: To achieve a reasonably large range for beam steering angle while using a small frequency change, we need to create large phase changes between the FSA radiating slots. To achieve this, our idea is to reduce the speed of the traveling wave inside the FSA. To control the speed of the wave, we build on a technique used in meta-materials, known as Spoof Surface Plasmon [30]. In particular, we place slots on the back of the FSA antenna. These back plate slots do not radiate the signal, but they act as a speed bump to reduce the wave velocity in the structure. Reducing the wave velocity provides a higher phase variation with frequency change, enabling larger beam steering angle in a smaller bandwidth.

(b) Covering negative angles: To enable beam steering for negative angles, we use modulated periodic slots on the top plate of our FSA. Specifically, as shown in Figure 5, the sizes of the radiating slots vary along the FSA structure. This periodicity in structure provides spatial amplitude modulation (AM) [2] of the wave in the FSA structure, which creates infinite number of space harmonics [12, 26, 66]. However, only the first harmonic radiates. This space harmonic creates negative phases for lower frequencies while positive phase for higher frequencies. Therefore, at the lower part of the frequency band, the FSA beam is pointing toward negative angles, while at higher frequencies, the beam is steered toward positive angles.

The design parameters to control the characteristics of the FSA are H_1, H_2, H_3, P, and d, as shown in Figure 5. As mentioned above, the slots in the back plane of the FSA do not radiate the signal. Rather, they are used to decrease the wave velocity. The proper wave velocity is achieved by adjusting the value of H_3 and d. For the slots in the top plane, the lengths of the slots are modulated. The period (P) and the amplitude of slots (H_1, H_2) define the backward and forward scanning range. Finally, the total number of slots and the length of the structure define the 3 dB beamwidth of the FSA.

3.2 2D Passive Beam Forming and Steering

In the previous section, we explained how we develop a passive structure for beamforming and steering in different

[2]Note spatial AM is different from temporal AM which is commonly used in wireless communication.

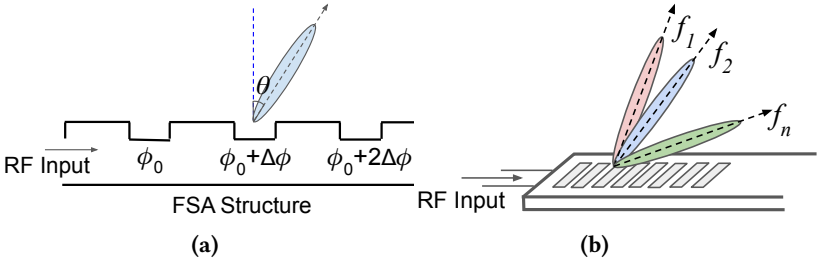

Figure 4: 1D Passive Beam forming and steering. The antenna fabricated on a thin PCB substrate (without any ICs) form a beam towards a direction that depends on the frequency of the transmitted or received signal. It can also create multiple beams towards different directions simultaneously.

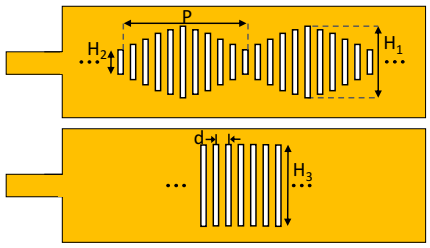

Figure 5: Our Designed FSA Antenna. The top and bottom layers of the antenna with modulated and equal length periodic slots, respectively.

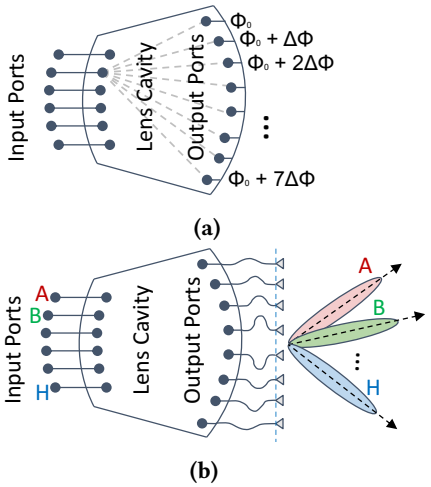

Figure 6: Rotman Lens. Rotmann Lens is passive structure which can be fabricated using just PCB. (a) It creates a specific phase change from each input port to the output port. (b) When the output ports are connected to individual antennas, it creates beams toward directions, depending on which input port is used. It can also create multiple beams simultaneously.

directions. However, since the proposed structure is a linear array of emitting elements, it forms beams only along a single dimension. To support multiple users in an area, our system needs to generate beams in 2D. Hence, the next question is how can we achieve passive 2D beamforming?

To address this question, our novel solution is to integrate our FSA design into a Rotman lens. Rotman lens is a passive structure mostly used in radar systems to detect targets in different directions [61]. The basic structure of the Rotman lens is shown in Figure 6. It consists of a number of input ports, a lens cavity, and a number of output ports which are typically connected to individual antennas. This structure can create a beam where its direction depends on which input port is used to feed the signal. The lens cavity, which can be fabricated using only a PCB, is designed such that it adds specific phase changes to the signal as it propagates from each input port of the Rotman lens to its output ports. Note, due to the shape of this structure, the amount of these phase changes depend on which input port is used for feeding the signal. Therefore, the antennas connected to the output ports of the Rotman lens emit the signal with different phases, creating a beam toward a direction that depends on which input port is used. Here, we explained how Rotman lens work for transmitting signals, it also works the same for receiving.

Note, both FSA and Rotman lens enables beam steering in only 1D. However, FSA steer the beam with change of frequency, and the Rotman lens steer the beam with change of input port. Hence, to enable 2D passive beamforming and steering, our idea is to develop a Rotman lens at mmWave and integrate it with our FSA design on the same PCB substrate, as shown in Figure 7. In particular, our design connects each output port of the Rotman lens to the input of a separate FSA structure instead of just a typical antenna. Below, we explain how this structure enables 2D beamforming and steering.

When a signal with a particular frequency is fed into one of the Rotman lens input ports, all FSAs receive the signal with different phase shifts created by Rotman lens cavity. Since the signal frequency is the same for all FSAs, they all create beams toward the same direction in 1D. However, since their signals have different phases caused by Rotman lens, their 1D beams are combined and create a 2D beam toward a specific direction. This novel structure enables passive beamforming and steering in 2D. In other words, by changing the frequency of the signal, we can steer the beam in one dimension, and by changing the input port which we feed the signal into Rotman lens, we can steer the beam in the other dimension. Thus, we can create multiple beams simultaneously in 2D by feeding signals of difference frequencies to different ports.

So far, we explained how to build a structure to perform 2D passive beam forming and steering. However, using this structure in a repeater requires selectively turning on/off each port using switches on the Rotman lens. Unfortunately, this solution requires feedback from the BS and client which is not ideal for a repeater. Another solution is to have the BS to steer its narrow beam only toward one of the input ports of the Rotman lens. However, this is not practical using

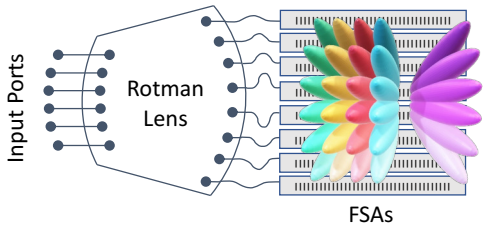

Figure 7: Our 2D Passive beam forming and steering. It can be fabricated on a thin PCB substrate (without any ICs) to passively form and steer narrow high-gain beams toward a direction that depends on which port and frequency is used. It can also create many beams simultaneously.

today's BS since their beams are not that narrow. To solve this challenge, in the next section, we propose to combine MU-MIMO and our structure to support multiple users in both dimension.

4 SUPPORTING MULTI-USER

So far, we have explained how we design a passive structure which can create and steer beams in 2D without consuming power or using any circuit components. Here, we explain how we use this structure to build a repeater which supports multiple users.

To build a repeater, we connect each input port of our passive structure shown in Figure 7 to a horn antenna. Such a design enables a repeater which can receive/transmit the signal from/to a base station using horn antennas and transmit/receive it to/from the clients using beams created by our passive structure. We are able to use horn antennas for backhaul (i.e. the link between the repeater and base station) since base stations and repeaters are typically fixed. Hence, they only need to perform the beam alignment process once, during the manual installation of the repeater. There are other alternative approaches for the backhaul link. These will be discussed in more detail in Section 8.

To support multi-user communication and steer its beam, mmXtend divides users into different frequency channels in one dimension using FSA beams. Hence, they can communicate simultaneously using Frequency Division Multiple Access (FDMA). To support multiple users in the other dimension, mmXtend divides users into different beams created by Rotman lens and use Multi-User Multiple Input Multiple Output (MU-MIMO), which is already provided in most mmWave base stations (such as 5G). Below we will first explain the basics of MU-MIMO, then we will explain how our design seamlessly operates in MU-MIMO scenarios.

4.1 MU-MIMO Integration

MU-MIMO enables a base station to simultaneously communicate to multiple users over the same frequency channel. In a typical MU-MIMO system (when there is no repeater),

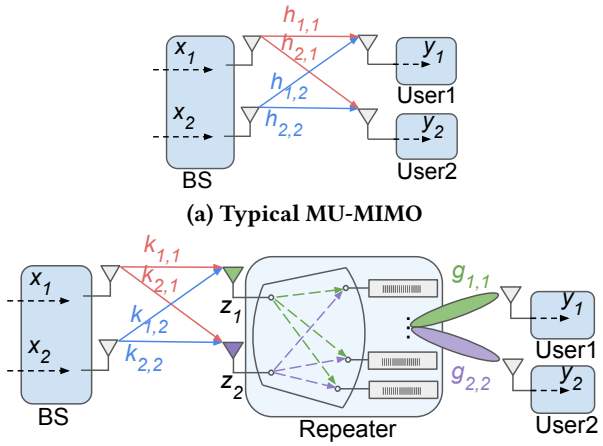

(a) Typical MU-MIMO

(b) MU- MIMO with mmXtend

Figure 8: MU-MIMO Examples. A typical 2×2 MU-MIMO system (a) without, and (b) with mmXtend's repeater.

the vector of received signals by users, y, can be written as follow: $y = HWx$, where H is the matrix of channels between the base station and users, W is the precoding matrix, and x is the vector of the data sent by the base station. Figure 8a shows an example of a typical 2×2 MU-MIMO. In these systems, the channel matrix H is measured in the channel estimation stage, and then the precoding matrix W is set to the inverse of the channel matrix. Hence, by transmitting Wx instead of x, the base station can simultaneously transmit multiple data streams while each user receives only its own data stream.

When we use our repeater in a typical MU-MIMO system as shown in Figure 8b, the only difference would be the channel matrix. The signals transmitted by the base station antennas will be first received by the backhaul antennas, and then they will be forwarded to users through separate beams created by the passive structure. Hence, the channel matrix will be $H = GK$, where K is the matrix of channels between the base station and the repeater's backhaul antennas, and G is the matrix of channels between the repeater and the user devices. Note, G is a diagonal matrix since the signal received at each backhaul antenna of the repeater creates a separate beam towards each user as shown in Figure 8b. To obtain the channel matrices, the base station and client perform their standard channel estimation through the reciprocal exchange of reference signals. For example, in the downlink, when the base station sends reference signal on a specific frequency channel, it will be received by the repeater and re-sent to different spatial directions. Users in each spatial direction will receive the signal, estimate the channel and send feedback. The same channel estimation process is done for each frequency channel. This works similarly for uplink channel estimation.

To enable MU-MIMO, the base station needs to set the precoding matrix W to the inverse of GK. Note that as our repeater is transparent to the base station and performs no processing on the signals, during the MU-MIMO channel estimation stage, the base station and users will measure GK as the channel matrix between the base station and users, and use it to compute the precoding matrix. The signals received by the backhaul antennas of the repeater can be presented as $z = KWx$, where $W = (GK)^{-1}$. Therefore, we can show that $z = G^{-1}x$. Note since G is a diagonal matrix, its inverse is also diagonal. This enables MU-MIMO from the base station to the repeater's backhaul antennas. Recall that the signal received at each repeater's backhaul antenna is directed toward a user via a beam using our repeater. Hence, the base station has supported MU-MIMO to the users without any additional complexity on the repeater [3]. Finally it is worth mentioning that here we focused on the downlink since the current implementation of our repeater, as described in section 6, is uni-directional. This limitation stems from the fact that LNAs used in our design are uni-directional. Hence, to send the channel estimation back to the base station from the user device or/and to support two-way communication, we need to use bidirectional LNAs or deploy two mmXtend repeaters.

5 NETWORK DETAILS

In the previous sections we presented the key components of mmXtend and explained how they are put together to enable a low-cost, low-power, on-demand repeater for mmWave networks. In this section we explain the networking details in using mmXtend in practice.

5.1 End-to-end Link Establishment

First, we explain how mmXtend establishes an end-to-end communication link between the base station (BS) and the user. In a typical mmWave network, the BS and the user need to perform beam searching to find the best direction for their beams to enable a communication path between the BS and the user [1, 54]. This path is typically the direct line-of-sight (LOS) path between them. Below we first explain how this process is done in today's 5G networks, and then describe how mmXtend's repeater can seamlessly be integrated without interfering with the standard process.

In the standard 5G mmWave beam alignment process, the BS sends groups of synchronization signals [2, 5] periodically in multiple spatial directions and different frequency channels, to detect users in different areas. On the user side, the user initiates a beam sweeping process using a wide beam and scans for available frequencies. It then reports to the BS which one of the BS's beams (i.e. frequency and direction) resulted in the highest received power [8, 59]. Based on the feedback from the user, the BS then aligns its beam direction to the user. Then the user begins beam sweeping using a narrow beam and aligns its beam toward the BS using received signal power measurements.

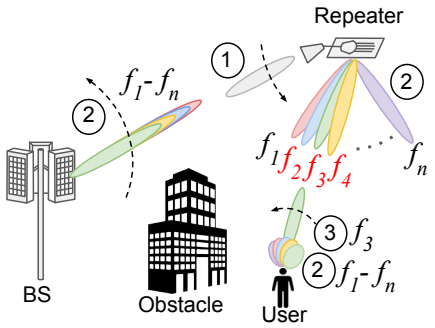

Figure 9: mmXtend Beam Alignment

When a mmXtend's repeater is installed and the LOS path is blocked, the BS and the user still tries to find the best communication path using the same standard process. Figure 9 shows the steps in end-to-end beam alignment when a repeater is deployed. In the first step, the repeater needs to have its backhaul beam aligned toward the BS. As mentioned before, the repeater is using fixed beam antennas (e.g. horn antenna) for its backhaul beams. Hence, during installation, the beams of the antennas can be manually adjusted toward the BS. Note, this is a one time process since the BS and repeater location is fixed in most scenarios. We will discuss alternative solutions for scenarios where the BS is mobile in Section 8. In the second step, the BS sweeps its beams and sends synchronization signals in multiple directions and frequency channels ($f_1 - f_n$). This process is the same as the standard 5G beam alignment process. However, when the beam of a particular frequency channel is steered in the direction of the repeater, its signal will be forwarded by the repeater to a specific direction based on its frequency. On the other side, the user also performs standard beam sweeping to find the direction and operating frequencies of the nearby base stations. The user provides feedback to the BS in the frequencies with the highest signal strength. This feedback will be transmitted back to the BS which allows it to determine which beam direction and which frequency provides the best performance for that user. This will be the direction which aligns the beam of the BS to the repeater, and the frequency which aligns the FSA beam to the user. This process will be repeated for each user. Note that in 5G FR2 mmWave bands, the same frequency channel is utilized for both uplink and downlink communication between a user and the BS through Time Division Duplexing (TDD) [7], so a user does not need to switch beams (frequencies) when transitioning between

[3]The Rotman lens acts as a spatial filter which facilitates MU-MIMO by splitting the signals through passive beamforming, creating a diagonal channel matrix between the repeater and the users. Without a Rotman lens, MU-MIMO will not be possible unless the additional signal processing is done on the repeater [51] which adds significant complexity and power consumption to the repeater system.

uplink and downlink communication. Finally, in the third step, the user performs the standard beam alignment process to find the best direction for its beam. This results in the alignment of the user's beam toward the repeater. After the beams are aligned, the user and the BS exchanges additional information to initiate downlink and uplink communication.

It worth mentioning that this entire process and all steps is done without the BS or user knowing there is a repeater. The repeater relays the signal between the BS and the user while the BS and user perform their standard 5G beam search process. Hence, mmXtend repeater can be seamlessly deployed wherever and whenever needed without requiring any cooperation or feedback from the BS or user.

5.2 Channel Resource Allocation

Next, we explain how mmXtend can provide opportunities for more flexible channel resource allocations to the users. In today's mmWave network, when we have a dense number of users in the same area, their network performance drops due to the sharing of the same frequency channel resource. In the design of mmXtend, we address this problem by providing partially overlapping channels of different frequencies to cover each area. As we mentioned earlier, our FSA shifts its beam continuously with respect to frequency. The scan ratio of our FSA design is 0.0167 degrees/MHz, meaning that for a channel bandwidth of 100 MHz and 400 MHz, the angle of the beam will shift by 1.67 degrees and 6.67 degrees, respectively. On top of this, we designed our FSA to achieve a 3 dB beamwidth of around 10 degrees for a single frequency. This means that the beamwidth of a single frequency is much larger than the amount of angle shift caused by the bandwidth of a frequency channel. Therefore, our design guarantees not only good coverage for each FSA beam, but also that each user will be covered by the FSA beams from a few different frequency channels.

This overlapping FSA beams provides an opportunity to enable more flexible channel resource allocation schemes for the users. In particular, the BS can allocate resource blocks based on the quality of each channel relative to the user location, as well as the occupancy of each channel. This enables more efficient bandwidth utilization of each channel when there are many users located in the same area, and ensures higher data rate for each user. When there are less number of users in each area, the overlapping channels also provides the opportunity to improve performance through carrier aggregation which is an existing feature in 5G networks [4].

Finally, in the case of user mobility, a user may move from one FSA beam to another beam. As the direction of the FSA beam is determined by the channel frequency, the operating channel of the user needs to be updated. Note that the BS is able to determine the best frequency channel to allocate to the user based on the continuous exchange of reference signals between the BS and the user, which are transmitted within the frequency of each channel on a periodic basis. Channel overlap in mmXtend, also enables a smoother hand-off process when the user moves between different channels, as the user can remain connected to a channel while initiate the hand-off procedure with adjacent channels at the same time. In particular, the BS dynamically adjusts the channel resources allocated to a user when it moves across different FSA beams. With the graceful hand-off process, the BS could schedule resources in advance in adjacent channels. As the repeater is mostly static, beam re-alignment from the base station to the repeater is rarely needed in the case of user mobility. In the rare case where the repeater moves (e.g. a drone repeater moving to a different height), the beam re-alignment between the base station and the repeater can be done with low delay. Beam scanning on the base station normally takes 5 ms (SSB burst), with an interval of 20 ms [65]. Furthermore, the SSB bursts can be sent simultaneously on different frequency channels depending on configuration. Hence beam re-alignment can be done with very low delay when the repeater moves.

5.3 Link Budget Analysis

In this section, we provide a link budget analysis for mmXtend. We only consider the downlink, where the base station is the transmitter and the user device is receiver. However, similar link budget calculation can be done for uplink too.

For our analysis, we calculate the SNR of the signal at the user device based on the following setup. We consider a typical 5G base station with an Effective Isotropic Radiated Power (EIRP) of 55 dBm [48], and a typical mmWave receiver with 20 dB antenna gain and noise floor of -88 dBm. We assume the repeater's backhaul antenna and each FSA has 20 dB and 10 dB gain, respectively, based on our measurement and simulation results presented in Sections 7.1. We consider the repeater's LNA gain and the number of FSAs as variables in our analysis. Finally, we assume that the distance of the mmXtend repeater is 200 meters from the base station, which is a reasonable distance to reach an outdoor base station to overcome signal blockage.

Figure 10a shows the SNR of the user versus distance of the user from the repeater. We plot the SNR for different number of FSA elements on the repeater where LNA gain is set to 20 dB. As the number of FSA elements increases, mmXtend enables higher SNR and/or longer communication range. However, as the number of FSA elements grows, the design becomes more complex. Hence, we fabricate a mmXtend repeater with eight FSA elements which is still easy to fabricate in a compact size while it provides SNR of 14 dB even when the user is 42 meters away from the repeater. Note, this SNR is sufficient to enable more than 240 Mbps data rate for a 100 MHz channel at 28 GHz.

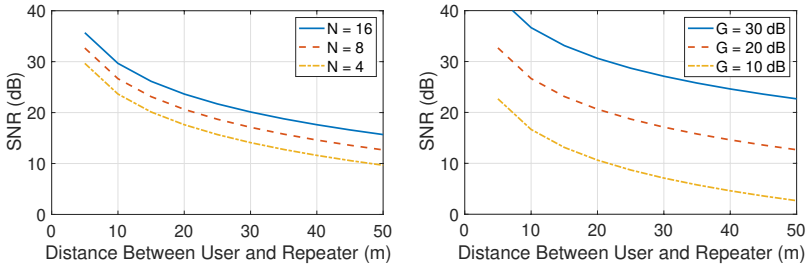

(a) (b)

Figure 10: Link Budget Analysis. SNR versus user to repeater distance when the repeater is 200 m away from the base station for (a) different number of FSA elements N, while the gain of the LNA is 20 dB, and (b) different LNA gains G, while the number of FSA elements is eight.

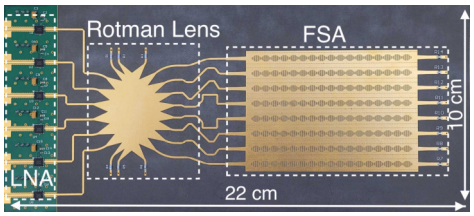

Figure 11: mmXtend Implementation. Our fabricated prototype on a thin and compact PCB substrate.

Figure 10b shows the SNR of the user versus distance of the user from the repeater. We plot the SNR for different LNA gain where we use eight FSA elements on the repeater. As the gain of the LNA increases, the communication range of mmXtend increases too. However, using higher LNA gains increases the power consumption of the repeater. Moreover, we cannot use very high-gain since at some point the gain becomes larger than the leakage between the repeater's backhaul and fronthaul beams, causing the self-interference problem. Hence, we fabricate a mmXtend's repeater using 20 dB LNAs. This enables mmXtend to achieve good communication range (i.e. SNR of 14 dB even at 42 meters) without having self-interference problem or consuming significant amount of power.

6 IMPLEMENTATION

To evaluate the performance of the mmXtend system, we have built a prototype of mmXtend. We have designed and implemented our prototype using high-frequency structure simulator (HFSS) software. Based on our link budget calculation in Section 5.3, we have designed a Rotman lens with eight outputs that connects to eight FSA elements. We integrated Rotman lens and FSAs on the same board and fabricated it in Rogers Duroid 5880 PCB substrate, as shown in Figure 11. Our prototype is only 22 cm by 10 cm and has a thickness of 0.5 mm. Our complete design operates in 5G 28 GHz mmWave band, and supports more than 3 GHz of bandwidth.

For backhaul antennas, we used Mi-Wave horn antennas (261-34-20-595), and connected them to the input port of our fabricated design. The combination of the horn antennas and FSA beams provides significant gain for our repeater. However, to provide further gain, we also placed a Low Noise Amplifier (LNA) between each horn antenna and our passive structure input ports. For LNAs, we have used HMC263LP4E from Analog Devices where each provides 20 dB LNA gain and consumes 174 mW of power. The LNAs are integrated on the same PCB board, as shown in Figure 11. Note, these six LNAs are the only components in our design which consumes power and the rest are passive.

7 EVALUATION

In this section, we present the performance of mmXtend under various conditions and scenarios. First, we investigate the radiation properties and scanning capability of mmXtend under microbenchmark testbeds. Then we explore the performance of mmXtend in extending mmWave coverage when the LOS between the base station and the user is blocked. We define different test scenarios and study the performance of the system (such as achievable SNR and data rate) in each case. We perform our experiments in both indoor and outdoor scenarios. We have used Keysight 5G R&D test bed [29] as our base station (BS) and user device to evaluate the performance of mmXtend. Our user device is equipped with a 20 dB gain antenna. Our base station is also equipped with a 20 dB gain antenna and uses transmission power of 35 dBm for both indoor and outdoor scenarios, which complies with FCC 5G 28 GHz band regulation [20]. Note, since our base station device supports only a single stream (i.e. does not support six parallel MIMO streams), our experiments are performed with a single antenna at a time.

7.1 Micro Benchmark

As discussed in Section 3.2, mmXtend forms and steers beams in 2D. In particular, mmXtend can steer its beam in one dimension by changing the signal frequency and in another dimension by using Rotman lens. Here, we evaluate mmXtend's capability to do so.

(a) FSA Beam Steering mmXtend designs FSAs to create and steer beams in the elevation plane. In particular, FSA steers its beam when the frequency of the signal changes. Here, we evaluate the performance our designed FSA to do this. Figure 12a shows the radiation pattern of our FSA as the signal frequency changes. For simplicity, the figure shows

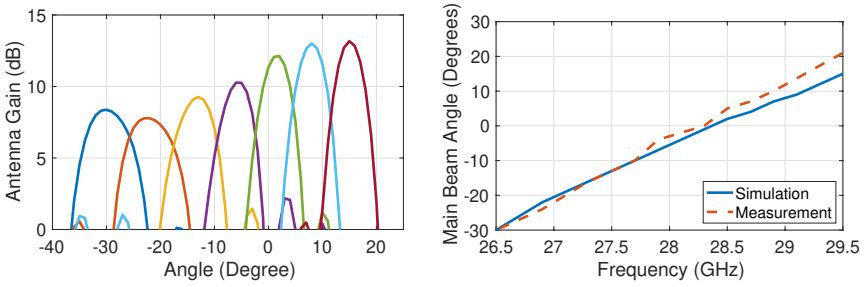

(a) (b)

Figure 12: FSA Beam Steering Performance. (a) Radiation pattern of the FSA for different signal frequencies. (b) FSA beam angle versus signal frequency.

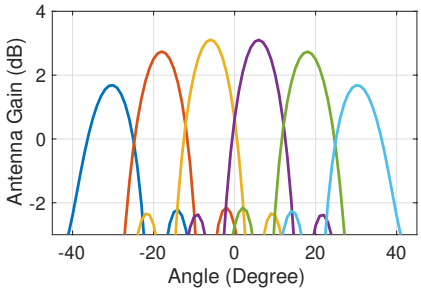

Figure 13: Rotman Lens Beam Steering Performance. Radiation pattern of our Rotman lens for different input ports.

the radiation pattern for seven different frequencies. However, it is worth mentioning that the FSA beam steering is continuous. The figure shows that our FSA design generates narrow beams with more than 8 dB gain. Moreover, the beam is steered as the frequency of the signal is changing. These results show that mmXtend can successfully form and steer multiple beams to multiple users by just using different signal frequencies. Figure 12b shows the relation between the direction of the beam and the frequency of the signal. This result implies that our design can steer its beams by more than 50 degrees by changing the frequency of the signal over the 5G mmWave band. Note repeaters are typically installed on a wall or ceiling and hence 50 degrees is enough to cover a large area. The figure also compares these results with the HFSS simulation results, implying that our fabricated prototype performance closely follows the expected results.

(b) Rotman Lens Beam Steering mmXtend designs a Rotman lens to steer its beam in the Azimuth plane. Here we evaluate the performance of our designed Rotman lens in creating and steering the beams. In particular, the Rotman lens steers its beam when different input ports are used for transmitting or receiving a signal. The radiation pattern of our designed Rotman lens is shown in Figure 13, where the vertical axis is the antenna gain in dB and the horizontal axis is the angle. The figure shows the radiation pattern for the six input ports of the Rotman lens. This result shows that our Rotman lens design is able to form narrow beams (with 1.5 to 2 dB gain) [4] in different directions while a different port is used. This meets our design goal of using Rotman lens as a spatial filter to enable multi-user access through multiple spatial beams in different directions. This Rotman lens can also create these beams simultaneously, spanning more than 65 degrees which in enough to cover a large area.

7.2 Angle Performance

So far we have evaluated the performance of individual components of mmXtend (i.e. our FSA and Rotman lens). Here, we evaluate the performance of the complete mmXtend in beamforming and repeating the signal toward a user, placed in different angles with respect to the repeater. We conducted this experiment in an indoor environment. We place the base station and repeater at fixed locations. We then place the user 3.5 meters away from the repeater and change its angle with respect to the user while measuring the SNR at the user. In particular, we are interested to see whether the repeater can steer its beam successfully toward the user (i.e. enabling reliable link without experiencing significant SNR drop) when the user is located at different azimuth and elevation angles. To examine only the effect of angle changes, we make sure that the distance of the user to the repeater is kept constant, and monitor the change in the SNR as we change azimuth and elevation angles of the user respect to the repeater. To steer the beam in the elevation angle, we transmitted signals of different frequencies ranging from 26.5 to 29.5 GHz. To steer the beam in the azimuth angle, we fed signal into each input port of the Rotman lens.

Figure 14a and 14b show the change in the SNR (with respect to the SNR at zero degree) for different azimuth and elevation angles of the user, respectively. The figures show that the repeater can steer its beam toward the user without significant SNR loss within the azimuth angle of -30 to 30 degrees and elevation angle of -40 to 40 degrees. Specifically, the worst SNR drop is 2 dB in elevation and 1 dB in azimuth plane. As we will show in the next evaluation, in most scenarios, mmXtend enables SNR of more than 20 dB, and hence a few dB drop in SNR will not have an impact on the achievable maximum data rate. Finally, considering that the repeaters are typically installed at a height (such as a pole, top of a building, or on a wall), the achieved angular range will be sufficient to cover a large area.

7.3 Range Performance

We evaluate the performance of mmXtend in solving the blockage problem and supporting reliable high SNR links in both indoor and outdoor scenario. We install our repeater at a fixed distance with respect to our base station, and measure

[4] Some possible approaches to improve the gain include increasing the number of ports, or developing substrate material with lower loss.

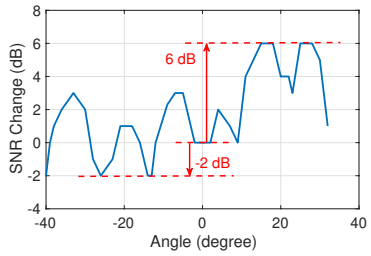

(a) Elevation Angle

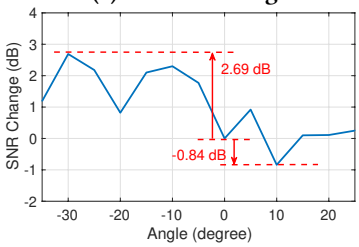

(b) Azimuth Angle

Figure 14: mmXtend Angle Performance. SNR change with respect to the SNR at zero degree.

the SNR of the signal received at the user placed at different distances with respect to the repeater. We connected one input port of the Rotman lens to a horn antenna for the backhaul link, and aligned the horn antenna to the remote base station. We make sure that the line-of-sight (LOS) path is always blocked, and the base station and the user communicate through our repeater.

a) Indoor Scenario mmXtend promises to enable reliable mmWave connectivity in indoor environments with blockages. Here, we verify if it delivers on this promise. We place a base station and a user device in our building where their LOS path is blocked by a concrete wall. We then place mmXtend in a position which has LOS to both the base station and user. The distance between the base station and repeater is eight meters while we change the distance between the user and repeater from 2 to 45 meters. For each distance, the base station is transmitting, and we measure the SNR at the user side. Note, since the LOS is blocked, the communication link is established through our repeater. Figure 15a shows the result of this experiment. The repeater has successfully enabled high SNR at the user. In particular, even when the user is 45 meters away from the repeater, the user still achieves more than 40 dB SNR. Note, SNR of more than 20 dB is sufficient to enable the maximum data rate in 5G networks. These results imply that mmXtend enables reliable high-data-rate wireless connectivity in indoor environment despite having blockage.

b) Outdoor Scenario. Next, we perform the same experiment as the previous one except in outdoor scenario. In this experiment, the base station and repeater are 170 meters apart.[5] We then place the user at different distances with respect to the repeater while its LOS path to the base station is always blocked. Figure 15b shows the achievable SNR of the user when we change the distance between the user and the repeater from 3 to 30 meters. The user has achieved the SNR of more than 20 dB in all locations. Such SNR is sufficient to enable the 5G maximum data rate. These results imply that mmXtend provides reliable high-data-rate wireless connectivity in outdoor environment, enabling emerging applications such as augmented sport and concert events, and autonomous robots to improve disaster recovery.

[5]The distance is limited by the space we had available for our tests.

7.4 Data Rate Performance

Next, we evaluate the performance of mmXtend in terms of user's data rate where multiple users seek communication with the base station via the repeater.

For this purpose, we use the following setup to conduct our evaluation. As shown in Figure 17, the repeater is placed on a pole at 14 meters above ground. The repeater establishes a backhaul link with a BS at 170 meters away while it relays the signal to cover a 2D plane on the ground noted by the x and y axis. Along the x axis, the plane is divided into 30 frequency channels, where each channel is covered by a single FSA beam (f_i). The bandwidth of each channel is 100 MHz, which corresponds to the 5G channel bandwidth [3, 48]. Along the y axis, the plane is divided into 6 sections, where each section is covered by a single Rotman lens beam (l_j). In total, it creates $30 \times 6 = 180$ cells. Users in different frequency cells (e.g. f_1 and f_2), communicate with the BS using different channels. For users located in the same frequency cell but different Rotman lens cells (e.g. (f_1, l_1) and (f_1, l_2)), they communicate with the BS through MU-MIMO in the same channel. If the users are in the same frequency cell and Rotman lens cell, the channel resource is shared through time-division multiple access. Finally, the coverage of mmXtend repeater along the x axis is 60 degrees and along the y axis is 72 degrees using FSA and Rotman lens, respectively.

To evaluate the performance of mmXtend in a network of users, we randomly distribute different number of users in the 2D plane covered by mmXtend and evaluate the average data rate of each user. To do so, since we do not have hundreds of user devices, we empirically measure the SNRs at different angles and distances (i.e. different cells) in our real-world experimental setup and use it to compute the data rate of each user in post-processing using the 5G mmWave NS3 simulator [6] [42]. Figure 16 shows the average user data rate with respect to the different number of users covered by the

[6]The BS communicates in the 5G NR frequency band of 26.5 to 29.5 GHz, the max downlink data rate per layer in a 100 MHz channel is 408 Mbps based on 3GPP standard [6]. For our evaluation, we assume the BS can provide the max data rate for all 30 channels in this spectrum at the same time. All six input ports of the Rotman lens is connected to the remote base station, enabling 6 data streams per frequency channel through MU-MIMO.

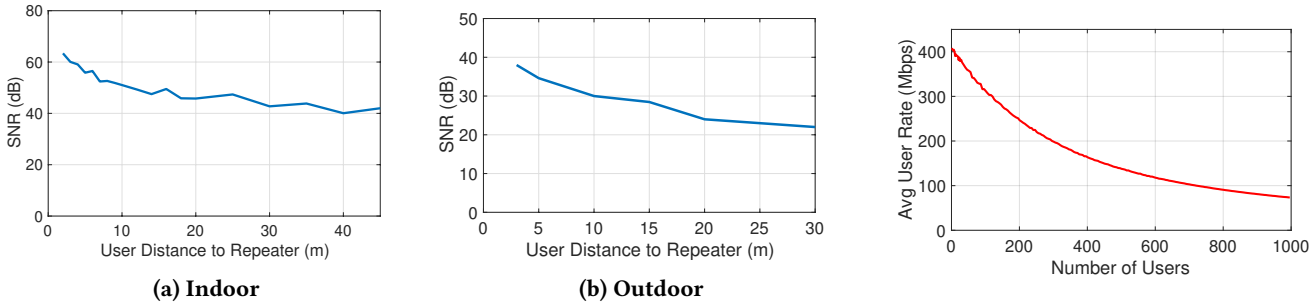

(a) Indoor (b) Outdoor

Figure 15: mmXtend Range Performance. (a) is an indoor scenario where the base station and the repeater are eight meters apart. (b) is an outdoor scenario where the base station and the repeater are 170 meters apart.

Figure 16: mmXtend Data Rate Performance. Average data rate per user versus different number of users.

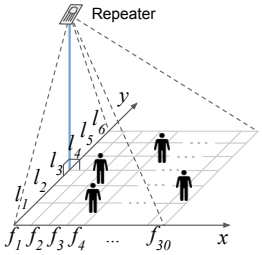

Figure 17: mmXtend Evaluation Setup. In the x axis, the area is divided into 30 channels covered by FSA beams, noted by f_1 to f_{30}. In the y axis, the area is divided into 6 sections covered by Rotman lens beams, noted by l_1 to l_6.

repeater. For each number of users, we ran our experiment 50 times with random distributions of users to calculate the average user data rate. The figure shows that when we have less than 100 users, the average data rate per user is as high as 300 to 400 Mbps. When the user number increases to 1000, we can still achieve an average user data rate of more than 70 Mbps. which is more than enough for streaming Ultra High Quality 4K videos. This result shows mmXtend's capability to provide high data rate links to a large number of users in a wide area when the LOS path between the user and the BS is blocked.

7.5 Power, Weight and Cost Analysis

The total power consumption of mmXtend is only 1.05 W which can be power up by a small solar panel (9×11 cm) [57] or a drone's battery without impacting on its flying time. Even small drones typically have batteries with 20-100 Wh capacity [16] which are not impacted by the low power consumption of mmXtend. Note, the total power consumption of mmXtend can be even further reduced to 300 mW by using recent released LNAs instead of the ones used in our prototype [15]. This power consumption is significantly lower than other technologies such as phased arrays and Reconfigurable Intelligent Surfaces (RIS). For example, mmWave phased arrays which offer similar gain and beamwidth, typically consume around 17 W [60, 64]. Similarly, typical RIS technologies consumes 5.3-8 W [24, 62], primarily due to their needs for Digital-to-Analog Converters (DACs) and high-speed control units, such as FPGAs.

Next, we compare the cost of mmXtend with existing solutions. mmXtend design includes a custom designed PCB, LNAs and horn antennas. Our mmXtend implementation (including 6 LNAs) as shown in figure 11, costs only $980. Note, this is the cost to fabricate one prototype device and hence it will be much lower in mass production. For comparison, the cost of the radio equipment for a commercial mmWave 5G base station typically exceeds $35,000 [19]. In comparison to passive reconfigurable metasurfaces, mmXtend also offers significant cost advantages. For instance, the surface design presented in [14] requires more than two thousands MAVR-011020-14110P Vractor Diodes (76 ribs, each consisting of 28 vertical meta-atoms) where each diode costs $2.5. Considering the cost of diodes, DACs and FPGA as well as the PCB fabrication and assembly costs, these surfaces cost $6,000 to $10,000 which is much higher than the cost of mmXtend.

Finally, it is worth mentioning that horn antenna and our 2D passive repeater structure (including 6 LNAs) weigh only 48.19 g and 70.02 g, respectively. Hence, our design is very light and can seamlessly be deployed on a pole or drone.

8 LIMITATIONS AND DISCUSSION

In this section we discuss some of the limitations of our design and propose potential solutions to enhance its applicability in real-world scenarios.

Backhaul Link: In the current design of mmXtend, we are using a fixed beam horn antenna for the backhaul link from the repeater to the base station since in most scenarios the base station is fixed. However, in some scenarios, the position of the base station may change, or the repeater may need to switch to a different base station. There are several possible approaches to address this challenge. First, the horn antennas could be connected to remote controlled gimbals, allowing adjustment to repeater's backhaul beam direction. Alternatively, we could use a passive multi-beam

design such as a Rotman lens or directional patch antennas for the backhaul link. This would enable the repeater to receive signals from base stations in varying directions and combine them to the input ports of mmXtend. This approach also enables the entire mmXtend design to be fabricated on a single PCB board.

Uplink Communication The current implementation of our repeater, detailed in Section 6, focuses on the downlink communication from the base station to the user since downlink is more important than uplink in most real time applications such as VR/AR. This uni-directional limitation stems from the fact that LNAs used in our design are unidirectional. Hence, to send the channel estimation back to the base station from the user device or/and to support two-way communication, we need to use bi-directional LNAs, or integrate LNAs in both directions for each input port of the Rotman lens. An alternative approach is to deploy two mmXtend repeaters, each dedicated to downlink or uplink communications.

9 RELATED WORK

In recent years, there has been a growing interest in solving the blockage problem in mmWave networks [14, 27, 46, 55, 56]. There are some works on building mmWave repeaters [9, 10, 22, 41, 43]. However, they either do not support multiple users or use complex, expensive, and power-hungry phased arrays. They also require significant feedback and cooperation with the base stations and users, to operate and keep its beams aligned toward users. Some recent work has proposed smart and intelligent surfaces [14, 23, 39, 45, 58]. These surfaces typically consist of a large array of passive elements which can reflect and refocus mmWave beams in certain directions passively. Although these systems do not need to use phased arrays, they are either non-reconfigurable [46] or require a large number of mmWave diodes (or varactors) and a processor such as FPGA to control individual elements, which makes the design complex and expensive. Moreover, they require feedback from the client and base station to operate and typically do not support multiple users simultaneously. In contrast, mmXtend introduces a mmWave repeater which supports multiple users, does not require any processor (such as FPGA), and does not require any feedback from the client or base station to operate. mmXtend achieves this by designing, building and integrating a passive 2D beamforming structure into mmWave repeaters.

Past work has explored passive 1D and 2D beamforming methods in the mmWave frequency. However, they all have certain limitations, and none of them targets repeater systems. For example, some past work has shown the potential of using Rotman lens for passive beamforming at mmWave frequencies [17, 18]. However, the only support 1D beamforming. Some other work has also proposed passive designs for 2D beamforming. However, these approaches [13, 31, 34] are very complex in design since they are interconnecting multiple layers of substrates in orthogonal planes. In contrast, our design is integrated into a single-layer substrate, which is compact, low cost, and easy to fabricate. It can be flexibly deployed at various locations on-demand. Finally, the authors in [68] proposed a 2D beam steering design using FSA and Rotman lens, however it is designed for near-field scenarios with limited coverage of tens of millimeters and FSA beam steering range of less than 25 degrees, which makes it impractical to be used for applications such as 5G communication, where a large number of users need to be covered in a large area. In contrast, our design can achieve a working distance of hundreds of meters and FSA beam steering range of more than 50 degrees. Moreover, we also incorporate Multi-User Multiple Input Multiple Output (MU-MIMO) enabling a repeater system which supports multiple users and works seamlessly with existing mmWave networks.

This paper is an extension of our previous workshop paper[33]. The workshop paper proposes only a 1D passive beamforming and steering structure using FSA, and shows its potential application in a mmWave repeater. That paper does not build the FSA, and provides only preliminary simulation results. In this paper, we introduce a 2D passive beamforming and steering structure. In particular, we develop a novel structure that consists of our designed Rotman lens and an array of FSAs to enable 2D passive beamforming. We also take into consideration actual design challenges for our design to work as a repeater in existing mmWave networks. In particular, using our passive 2D beamforming structure and off-the-shelf components, we then build a complete repeater capable of supporting multiple users. Finally, we run experiments and empirically evaluate the end-to-end performance of our system in different scenarios.

10 CONCLUSION

This paper presents mmXtend, an on-demand repeater which solves the blockage problem of mmWave networks in outdoor and indoor scenarios. mmXtend is low cost, low power, and can be seamlessly deployed whenever and wherever is needed. We achieve this by introducing a novel design which enables the repeater to passively create and steer beams to multiple users simultaneously. Finally, we implemented mmXtend and empirically evaluated its performance mmXtend enables reliable high-data-rate connectivity to hundreds of users even when they are hundreds of meters away from the base station and their line-of-sight path to it is blocked.

ACKNOWLEDGMENTS

We thank the anonymous reviewers for their valuable feedback on this paper. We thank UCLA and NSF for their partial support.

REFERENCES

[1] 3GPP. 2017. 3GPP TR 38.802 Release 14 - 6.1.6.1 Beam Management. https://www.3gpp.org/ftp/Specs/archive/38_series/38.802/.

[2] 3GPP. 2017. 3GPP TR 38.802 Release 14 - 6.2.3.1 Synchronization signal and DL broadcast signal/channel structure. https://www.3gpp.org/ftp/Specs/archive/38_series/38.802/.

[3] 3GPP. 2021. 3GPP TS 38.104 Release 17 - 5.2, 5.3 Operating bands and channel bandwidth. https://www.3gpp.org/ftp/Specs/archive/38_series/38.104/.

[4] 3GPP. 2021. 3GPP TS 38.104 Release 17 - 5.3A BS channel bandwidth for CA. https://www.3gpp.org/ftp/Specs/archive/38_series/38.104/.

[5] 3GPP. 2021. 3GPP TS 38.104 Release 17 - 5.4.3 Synchronization Raster. https://www.3gpp.org/ftp/Specs/archive/38_series/38.104/.

[6] 3GPP. 2022. 3GPP TS 38.306 V17.3.0 - 5 UE radio access capability parameters. https://www.3gpp.org/ftp/Specs/archive/38_series/38.306/.

[7] 3GPP. 2023. 3GPP TS 38.101-2 Release 18 - 5.2 Operating Bands. https://www.3gpp.org/ftp/Specs/archive/38_series/38.101-2/.

[8] 5GWorldPro.com. 2020. What are 5G Beam management procedures. https://www.5gworldpro.com/5g-knowledge/what-are-5g-beam-management-procedures.html.

[9] Omid Abari, Dinesh Bharadia, Austin Duffield, and Dina Katabi. 2016. Cutting the cord in virtual reality. In *Proceedings of the 15th ACM Workshop on Hot Topics in Networks*. 162–168.

[10] Omid Abari, Dinesh Bharadia, Austin Duffield, and Dina Katabi. 2017. Enabling high-quality untethered virtual reality. In *14th {USENIX} Symposium on Networked Systems Design and Implementation ({NSDI} 17)*. 531–544.

[11] Cooley Alert. 2016. FCC Opens Millimeter Wave Spectrum for 5G. https://www.cooley.com/news/insight/2016/2016-07-14-fcc-opens-millimeter-wave-spectrum-for-5g.

[12] Leon Brillouin. 1953. *Wave propagation in periodic structures: electric filters and crystal lattices*. Vol. 2. Dover publications.

[13] René Camblor, Samuel Ver Hoeye, Miguel Fernandez, Carlos Vázquez Antuña, and Fernando Las-Heras. 2017. Full 2-D submillimeter-wave frequency scanning array. *IEEE Transactions on Antennas and Propagation* 65, 9 (2017), 4486–4494.

[14] Kun Woo Cho, Mohammad H Mazaheri, Jeremy Gummeson, Omid Abari, and Kyle Jamieson. 2023. {mmWall}: A Steerable, Transflective Metamaterial Surface for {NextG}{mmWave} Networks. In *20th USENIX Symposium on Networked Systems Design and Implementation (NSDI 23)*. 1647–1665.

[15] Analog Devices. 2022. ADL8142: GaAs, pHEMT, MMIC, Low Noise Amplifier, 23 GHz to 31 GHz Data Sheet (Rev. A). https://www.analog.com/media/en/technical-documentation/data-sheets/adl8142.pdf.

[16] DJI. 2023. DJI Consumer Drones Comparison. https://www.dji.com/products/comparison-consumer-drones.

[17] Aline Eid, Jimmy GD Hester, and Manos M Tentzeris. 2020. Rotman lens-based wide angular coverage and high-gain semipassive architecture for ultralong range mm-wave RFIDs. *IEEE Antennas and Wireless Propagation Letters* 19, 11 (2020), 1943–1947.

[18] Aline Eid, Jimmy GD Hester, and Manos M Tentzeris. 2021. 5G as a wireless power grid. *Scientific Reports* 11, 1 (2021), 636.

[19] Mobile Experts. 2021. White Paper: 5G mmWave Repeaters Cut Costs in Half. https://mobile-experts.net/reports/p/white-paper-semiconductors-for-oran-ss6db.

[20] FCC. 2023. FCC mmWave Transmit Power Regulation. https://www.ecfr.gov/current/title-47/chapter-I/subchapter-B/part-30.

[21] Valerio Frascolla, Federico Miatton, Gia Khanh Tran, Koji Takinami, Antonio De Domenico, Emilio Calvanese Strinati, Konstantin Koslowski, Thomas Haustein, Kei Sakaguchi, Sergio Barbarossa, et al. 2017. 5G-MiEdge: Design, standardization and deployment of 5G phase II technologies: MEC and mmWaves joint development for Tokyo 2020 Olympic games. In *2017 IEEE Conference on Standards for Communications and Networking (CSCN)*. IEEE, 54–59.

[22] FRTek. 2022. FRTek 28GHz 5G Wireless Optical Distributed Repeater. http://www.frtek.com/en/board/board.php?bo_table=wireless&cate=DAS&idx=101.

[23] Jean-Baptiste Gros, Vladislav Popov, Mikhail A Odit, Vladimir Lenets, and Geoffroy Lerosey. 2021. A reconfigurable intelligent surface at mmWave based on a binary phase tunable metasurface. *IEEE Open Journal of the Communications Society* 2 (2021), 1055–1064.

[24] Jean-Baptiste Gros, Vladislav Popov, Mikhail A Odit, Vladimir Lenets, and Geoffroy Lerosey. 2021. A reconfigurable intelligent surface at mmWave based on a binary phase tunable metasurface. *IEEE Open Journal of the Communications Society* 2 (2021), 1055–1064.

[25] Haitham Hassanieh, Omid Abari, Michael Rodriguez, Mohammed Abdelghany, Dina Katabi, and Piotr Indyk. 2018. Fast millimeter wave beam alignment. In *Proceedings of the 2018 Conference of the ACM Special Interest Group on Data Communication*. 432–445.

[26] Tatsuo Itoh. 2004. Periodic structures for microwave engineering. In *MWE Microw. Workshop*.

[27] Suraj Jog, Jiaming Wang, Junfeng Guan, Thomas Moon, Haitham Hassanieh, and Romit Roy Choudhury. 2019. {Many-to-Many} Beam Alignment in Millimeter Wave Networks. In *16th USENIX Symposium on Networked Systems Design and Implementation (NSDI 19)*. 783–800.

[28] Shaya Karimkashi and Guifu Zhang. 2013. A dual-polarized series-fed microstrip antenna array with very high polarization purity for weather measurements. *IEEE transactions on antennas and propagation* 61, 10 (2013), 5315–5319.

[29] Keysight. 2023. Keysight 5G NR R&D Testbed. https://www.keysight.com/us/en/products/modular/reference-solutions/5g-waveform-generation-analysis-testbed-reference-solution.html.

[30] Amin Kianinejad, Zhi Ning Chen, and Cheng-Wei Qiu. 2016. Low-loss spoof surface plasmon slow-wave transmission lines with compact transition and high isolation. *IEEE Transactions on Microwave Theory and Techniques* 64, 10 (2016), 3078–3086.

[31] Weiyang Kong, Yun Hu, Jiawang Li, Lei Zhang, and Wei Hong. 2022. 2-D Orthogonal Multibeam Antenna Arrays for 5G Millimeter-Wave Applications. *IEEE Transactions on Microwave Theory and Techniques* 70, 5 (2022), 2815–2824.

[32] Bin Li, Zheng Zhou, Weixia Zou, Xuebin Sun, and Guanglong Du. 2012. On the efficient beam-forming training for 60GHz wireless personal area networks. *IEEE Transactions on Wireless Communications* 12, 2 (2012), 504–515.

[33] Tianxiang Li, Mohammad Hossein Mazaheri, and Omid Abari. 2022. 5g in the sky: the future of high-speed internet via unmanned aerial vehicles. In *Proceedings of the 23rd Annual International Workshop on Mobile Computing Systems and Applications*. 116–122.

[34] Yujian Li, Junhong Wang, and Kwai-Man Luk. 2017. Millimeter-wave multibeam aperture-coupled magnetoelectric dipole array with planar substrate integrated beamforming network for 5G applications. *IEEE transactions on antennas and propagation* 65, 12 (2017), 6422–6431.

[35] Haofan Lu, Mohammad Mazaheri, Reza Rezvani, and Omid Abari. 2023. A Millimeter Wave Backscatter Network for Two-Way Communication and Localization. In *Proceedings of the ACM SIGCOMM 2023 Conference*. 49–61.

[36] Mohammad Mazaheri, Rafael Ruiz, Domenico Giustiniano, Joerg Widmer, and Omid Abari. 2023. Bringing Millimeter Wave Technology to Any IoT Device. In *Proceedings of the 29th Annual International Conference on Mobile Computing and Networking*. 1–15.

[37] Mohammad H Mazaheri, Soroush Ameli, Ali Abedi, and Omid Abari. 2019. A millimeter wave network for billions of things. In *Proceedings*

of the ACM Special Interest Group on Data Communication. 174–186.

[38] Mohammad Hossein Mazaheri, Alex Chen, and Omid Abari. 2021. mmTag: a millimeter wave backscatter network. In *Proceedings of the 2021 ACM SIGCOMM 2021 Conference*. 463–474.

[39] Metawave. 2018. Successful Demonstration of 28GHz-Band 5G Using World's First Meta-Structure Technology. https://www.metawave.com/post/successful-demonstration-of-28ghz-band-5g-using-world-s-first-meta-structure-technology.

[40] Metawave. 2020. MIRAIT and METAWAVE conducted indoor demonstration test of ECHO using metamaterial tech for 5G. https://www.metawave.com/post/mirait-and-metawave-conducted-indoor-demonstration-test-of-echo-using-metamaterial-tech-for-5g.

[41] Metawave. 2021. Metawave Turbo. https://www.metawave.com/post/metawave-selects-analog-devices-beamforming-technology-for-turbo-5g-repeater.

[42] Marco Mezzavilla et al. 2018. End-to-end simulation of 5G mmWave networks. *IEEE Communications Surveys & Tutorials* 20, 3 (2018), 2237–2263.

[43] movandi. [n. d.]. Movandi 5G Repeaters. https://movandi.com/smart-repeaters/.

[44] Zhouyue Pi and Farooq Khan. 2011. An introduction to millimeter-wave mobile broadband systems. *IEEE communications magazine* 49, 6 (2011), 101–107.

[45] Chandan Pradhan, Ang Li, Lingyang Song, Branka Vucetic, and Yonghui Li. 2020. Hybrid precoding design for reconfigurable intelligent surface aided mmWave communication systems. *IEEE Wireless Communications Letters* 9, 7 (2020), 1041–1045.

[46] Kun Qian, Lulu Yao, Xinyu Zhang, and Tse Nga Ng. 2022. MilliMirror: 3D printed reflecting surface for millimeter-wave coverage expansion. In *Proceedings of the 28th Annual International Conference on Mobile Computing And Networking*. 15–28.

[47] Qualcomm. 2018. VR and AR pushing connectivity limits. https://www.qualcomm.com/media/documents/files/vr-and-ar-pushing-connectivity-limits.pdf.

[48] Qualcomm. 2019. 5G NR mmWave outdoor and indoor deployment strategy. https://www.qualcomm.com/media/documents/files/deploying-5g-nr-mmwave-for-indoor-outdoor.pdf.

[49] Sundeep Rangan, Theodore S Rappaport, and Elza Erkip. 2014. Millimeter-wave cellular wireless networks: Potentials and challenges. *Proc. IEEE* 102, 3 (2014), 366–385.

[50] Theodore S Rappaport, Shu Sun, Rimma Mayzus, Hang Zhao, Yaniv Azar, Kevin Wang, George N Wong, Jocelyn K Schulz, Mathew Samimi, and Felix Gutierrez. 2013. Millimeter wave mobile communications for 5G cellular: It will work! *IEEE access* 1 (2013), 335–349.

[51] Umar Rashid, Hoang Duong Tuan, Ha Hoang Kha, and Ha H Nguyen. 2014. Joint optimization of source precoding and relay beamforming in wireless MIMO relay networks. *IEEE Transactions on communications* 62, 2 (2014), 488–499.

[52] Pei Ren, Xiuquan Qiao, Yakun Huang, Ling Liu, Schahram Dustdar, and Junliang Chen. 2020. Edge-assisted distributed DNN collaborative computing approach for mobile web augmented reality in 5G networks. *IEEE Network* 34, 2 (2020), 254–261.

[53] Stefano Savazzi, Monica Nicoli, and Vittorio Rampa. 2020. Federated learning with cooperating devices: A consensus approach for massive IoT networks. *IEEE Internet of Things Journal* 7, 5 (2020), 4641–4654.

[54] ShareTechnote.com. 2022. 5G/NR - Beam Management. https://www.sharetechnote.com/html/5G/5G_Phy_BeamManagement.html.

[55] Sanjib Sur, Ioannis Pefkianakis, Xinyu Zhang, and Kyu-Han Kim. 2018. Towards scalable and ubiquitous millimeter-wave wireless networks. In *Proceedings of the 24th Annual International Conference on Mobile Computing and Networking*. 257–271.

[56] Sanjib Sur, Xinyu Zhang, Parmesh Ramanathan, and Ranveer Chandra. 2016. BeamSpy: Enabling robust 60 GHz links under blockage. In *13th {USENIX} Symposium on Networked Systems Design and Implementation ({NSDI} 16)*. 193–206.

[57] Voltaic Systems. 2023. 1 Watt 6 Volt Solar Panel. https://voltaicsystems.com/1-watt-panel/.

[58] Xin Tan, Zhi Sun, Dimitrios Koutsonikolas, and Josep M Jornet. 2018. Enabling indoor mobile millimeter-wave networks based on smart reflect-arrays. In *IEEE INFOCOM 2018-IEEE Conference on Computer Communications*. IEEE, 270–278.

[59] Tweet4Technology.com. 2022. 5G NR: 5G-NR Cell Search Procedure. https://tweet4technology.blogspot.com/2019/10/5g-cell-search-procedure.html.

[60] Risto Valkonen. 2018. Compact 28-GHz phased array antenna for 5G access. In *2018 IEEE/MTT-S International Microwave Symposium-IMS*. IEEE, 1334–1337.

[61] Shruti Vashist, MK Soni, and PK Singhal. 2014. A review on the development of Rotman lens antenna. *Chinese Journal of Engineering* 2014, 11 (2014), 1–9.

[62] Xiang Wan, Qiang Xiao, Ying Zhe Zhang, Yueheng Li, Joerg Eisenbeis, Jia Wei Wang, Zi Ai Huang, Han Xiao Liu, Thomas Zwick, and Tie Jun Cui. 2021. Reconfigurable sum and difference beams based on a binary programmable metasurface. *IEEE Antennas and Wireless Propagation Letters* 20, 3 (2021), 381–385.

[63] Xiaoli Wang, Aakanksha Chowdhery, and Mung Chiang. 2017. Networked drone cameras for sports streaming. In *2017 IEEE 37th International Conference on Distributed Computing Systems (ICDCS)*. IEEE, 308–318.

[64] Extreme Waves. 2022. Extreme Waves mmWave Phased Array Repeaters. https://www.extreme-waves.com/5g.

[65] RF Wireless World. [n. d.]. What Is 5G NR SS Block | SS Burst Vs SS Block. https://www.rfwireless-world.com/5G/5G-NR-SS-Block.html.

[66] Geng-Bo Wu, Qing-Le Zhang, Ka Fai Chan, Bao-Jie Chen, and Chi Hou Chan. 2020. Amplitude-modulated leaky-wave antennas. *IEEE Transactions on Antennas and Propagation* 69, 7 (2020), 3664–3676.

[67] Wen Wu, Nan Cheng, Ning Zhang, Peng Yang, Weihua Zhuang, and Xuemin Shen. 2019. Fast mmwave beam alignment via correlated bandit learning. *IEEE Transactions on Wireless Communications* 18, 12 (2019), 5894–5908.

[68] Ya Fei Wu, Yu Jian Cheng, and Zi Xuan Huang. 2018. Ka-band near-field-focused 2-D steering antenna array with a focused Rotman lens. *IEEE Transactions on Antennas and Propagation* 66, 10 (2018), 5204–5213.

[69] Sun Zhan-shan, Ren Ke, Chen Qiang, Bai Jia-jun, and Fu Yun-qi. 2017. 3D radar imaging based on frequency-scanned antenna. *IEICE Electronics Express* 14, 12 (2017), 20170503–20170503.

[70] Hang Zhao et al. 2013. 28 GHz millimeter wave cellular communication measurements for reflection and penetration loss in and around buildings in New York city. In *2013 IEEE international conference on communications (ICC)*. IEEE, 5163–5167.

[71] Guangxu Zhu, Yong Wang, and Kaibin Huang. 2019. Broadband analog aggregation for low-latency federated edge learning. *IEEE Transactions on Wireless Communications* 19, 1 (2019), 491–506.